J. exp. Biol. 151, 387–403 (1990)
Printed in Great Britain © The Company of Biologists Limited 1990

PATCH-CLAMP STUDY OF THE PROPERTIES OF THE SODIUM CURRENT IN COCKROACH SINGLE ISOLATED ADULT AMINERGIC NEURONES

BY BRUNO LAPIED*, CLAIRE O. MALÉCOT AND MARCEL PELHATE

Laboratoire de Neurophysiologie, CNRS URA 611, Université d'Angers, rue Haute-de-Reculée, F-49045 Angers Cedex, France

Accepted 27 February 1990

Summary

The properties of the fast Na^+ inward current of the aminergic neurosecretory dorsal unpaired median (DUM) cells isolated from the sixth abdominal ganglion of the cockroach *Periplaneta americana* were studied with the whole-cell clamp technique in the presence of Ca^{2+} and K^+ channel blockers. In about 80 % of the cells, the current activated at −35 mV, was maximal at −10 mV and reversed at +48 mV (V_{rev}), very close to V_{Na}, the equilibrium potential for Na^+ (+47.9 mV). V_{rev} followed V_{Na} when the external Na^+ concentration was varied and the current was entirely suppressed by 1.0×10^{-7} mol l^{-1} saxitoxin (STX), indicating that it was carried by Na^+. In the remaining cells, an STX-sensitive maintained current was observed, the peak current–voltage relationship having almost the same characteristics except that an additional small shoulder was present between −90 and −35 mV, suggesting the existence of two types of Na^+ channels. Na^+ channels were half-inactivated at −41.1 mV and half-activated at −25.8 mV. The overlap of inactivation (h_∞) and activation (m_∞) parameters was important (−70 to +10 mV). h_∞ was not well fitted by a single Boltzmann distribution for potentials more negative than −70 mV, indicating more than one process of inactivation. The half-times of activation and of inactivation of the Na^+ current were voltage-dependent, strongly decreasing with increasing pulse amplitude. The time courses of both inactivation and recovery from inactivation were best described by the sum of two exponentials. The two components of inactivation did not contribute equally to the decay of the current; the fast component accounting for more than 90 % of the inactivation at positive potentials. Taken together, the results suggest that the Na^+ channels of DUM neurones have more than one open state and/or more than one inactivated state.

Introduction

Using different staining methods and electrophysiological techniques, a small

*To whom reprint requests should be sent.

Key words: patch-clamp, voltage-clamp, Na^+ current, cockroach, adult isolated DUM neurones, A6 ganglion.

population of typical nerve cell bodies can be identified along the dorsal median line of ganglia along the nerve cord of the central nervous system of most insects; for this reason the cells are called the dorsal unpaired median (DUM) cells.

The DUM cells, first described by Plotnikova (1969) and whose structure has mainly been studied in the locust (Watson, 1984; Pflüger and Watson, 1988), make a T-branch with symmetrical axons running into the left and right sides of the ganglion to innervate the peripheral structures. These neurones are capable of generating typical electrical activity. For example, spontaneous overshooting fast action potentials have been recorded from the soma near the dorsal surface of the locust thoracic ganglia (Hoyle and Dagan, 1978; Goodman and Spitzer, 1981*a*,*b*) and in the cockroach metathoracic and abdominal ganglia (Kerkut *et al.* 1969; Jego *et al.* 1970; Crossman *et al.* 1971; Lapied *et al.* 1989).

In situ intracellular microelectrode investigations have shown that the physiological role of the DUM neurones was directly or indirectly to modulate the activity of skeletal muscle (e.g. the DUMETi in locust metathoracic ganglia, Hoyle, 1975; Evans and O'Shea, 1978; O'Shea and Evans, 1979; the DUM3,5,6 in the cockroach metathoracic ganglia, Tanaka and Washio, 1988) or that of visceral muscle (e.g. the DUMOV1–2 in the locust abdominal ganglia, Lange and Orchard, 1984). Another characteristic of the DUM cells is that they have been shown, in general, to contain a biogenic amine, octopamine (Hoyle, 1975; Evans and O'Shea, 1978; Dymond and Evans, 1979; Konings *et al.* 1988) and, therefore, it has been suggested that their function might be neurosecretory.

Thus, these aminergic neurones could be a suitable model to investigate the physiological processes involved in excitation–secretion coupling and in the regulation of neurosecretory functions. However, before studying these complex mechanisms, it appeared essential to determine precisely the basic ionic mechanisms involved in their spontaneous electrical activity. Further understanding of the properties of the excitable membrane of these neurones can be obtained with the patch-clamp technique after dissociation of the dorsal side of the sixth abdominal (A6) ganglion of the cockroach. With this method, we have shown in a previous paper (Lapied *et al.* 1989) that the characteristics of the electrical activity of the isolated neurones were similar to those of the neurones studied *in situ* with the intracellular microelectrode technique. This confirmed that the spontaneous activity was an intrinsic property of the soma. Furthermore, it has been established that sodium ions were responsible for the depolarizing phase of the action potentials.

So far, the studies have mostly been carried out on the thoracic ganglia of a number of insect species but almost nothing is known concerning the specific physiological role of the DUM cells in the abdominal ganglia, especially in the cockroach. Moreover, apart from a voltage-clamp study of a calcium-activated potassium conductance (Thomas, 1984) and a patch-clamp study of unitary potassium currents (Dunbar and Pitman, 1985) in the cockroach thoracic ganglion, the characteristics of the ionic currents underlying the spontaneous action potentials have not yet been determined. Therefore, it appeared necessary to

characterize the kinetics of the other ionic currents and, above all, those of the sodium current.

In this paper, we describe the first detailed study with the patch-clamp technique of the voltage-dependent inward sodium current involved in the electrical activity of the isolated DUM cells present in the A6 ganglion of the cockroach.

Materials and methods

Adult male cockroaches (*Periplaneta americana* L.), reared at 29°C in the laboratory, were used. Electrophysiological recordings were made from the somata of a small population (about 40 cells) of neurones (called the DUM cells) situated along the dorsal midline of the sixth abdominal (A6) ganglion of the nerve cord (for details, see Dymond and Evans, 1979).

Cell isolation

Nerve cell bodies from the A6 ganglion were prepared under sterile conditions according to a modified version of the technique of Pinnock and Sattelle (1987). Briefly, after isolation of the abdominal nerve cord, the A6 ganglia were desheathed and the dorsal median parts were incubated for 1 h in normal saline containing collagenase (type IA, $1\,mg\,ml^{-1}$) and hyaluronidase (type IS, $2\,mg\,ml^{-1}$). The ganglia were then rinsed in normal saline and mechanically dissociated by repetitive gentle suctions through a Pasteur pipette. Cells were allowed to settle on poly-D-lysine (poly-D-lysine hydrobromide, M_r 70000–150000) coating the bottom of a Petri dish filled with normal saline supplemented with foetal calf serum (FCS, 5% by volume) and gentamycin ($20\,\mu g\,ml^{-1}$). All compounds were obtained from Sigma Chemicals (L'Isle d'Abeau Chesnes, France) except FCS (GIBCO, Cergy Pontoise, France). The neurones used in the present study were chosen as previously described (Lapied *et al.* 1989).

Solutions

The normal saline for cell isolation contained (in $mmol\,l^{-1}$): NaCl, 200; KCl, 3.1; $CaCl_2$, 5; $MgCl_2$, 4; sucrose, 50; Hepes buffer, 10; pH adjusted to 7.4 with NaOH. For the experiments, the saline superfusing the cells contained (in mmol l^{-1}): NaCl, 100; tetraethylammonium chloride (TEACl), 100; KCl, 3.1; $CaCl_2$, 2; $MgCl_2$, 7; $NiCl_2$, 0.1; 4-aminopyridine, 1; (±)-verapamil, 0.01; Hepes buffer, 10; pH adjusted to 7.4 with TEAOH. For experiments carried out in a low- or in a high-Na^+ medium, TEA^+ concentration was varied accordingly to keep the total concentration of NaCl and TEA^+ to $200\,mmol\,l^{-1}$. The internal solution in the recording pipette contained (in $mmol\,l^{-1}$): CsCl, 70; CsF, 70; NaCl, 15; $MgCl_2$, 1; EGTA, 5; ATP–Mg, 2; Hepes buffer, 10; pH adjusted to 7.4 with CsOH. During the course of the experiments, the saline superfusing the cell under study was delivered close to the cell through a gravity perfusion system, allowing complete solution changes within less than 3 s. When needed, synthetic saxitoxin (STX) was

added to the superfusing saline at a concentration of 1.0×10^{-7} mol l^{-1}. Experiments were carried out at room temperature (20°C).

Electrophysiological recordings and data analysis

Membrane currents were recorded with the patch-clamp technique (Hamill *et al.* 1981) in the whole-cell configuration. Patch electrodes were pulled from borosilicate capillary tubes (Clark Electromedical Instruments, Reading, UK) with a BB-CH puller (Mecanex, Geneva, Switzerland) and had resistances of 0.9–1.3 MΩ when filled with the pipette solution. Liquid junction potential between the pipette and the superfusing solutions was always corrected before formation of a seal of at least 2 GΩ.

Membrane potential was controlled by applying voltage to the interior of the pipette with a patch-clamp amplifier (RK 300: Biologic, Echirolles, France). Cells were clamped at a holding potential of −100 mV, and test pulses of 50 ms in duration, except where otherwise stated, were applied at 0.5 Hz either with a programmable stimulator (SMP 300: Biologic, Echirolles, France) or with pClamp version 5.03 software (Axon Instruments Inc., Foster City, CA, USA) running on a Compaq Deskpro 286 computer connected to a 125 kHz Labmaster DMA data acquisition system (TL–1–125 interface: Axon Instruments Inc., Foster City, CA, USA). Series resistance values were obtained for each experiment from the patch-clamp amplifier settings after compensation and varied between 2 and 6 MΩ. Because the neurones studied were relatively large (40–60 μm in diameter), their membrane capacitances were high (200–400 pF). Therefore, the adequacy of the voltage-clamp was assessed by measuring the cell potential directly with a conventional intracellular microelectrode (tip resistance 30 MΩ when filled with 3 mol l^{-1} KCl) connected to a VF-180 microelectrode amplifier (Biologic, Echirolles, France). In none of the experiments did the cell potential differ from the pipette potential by more than 2 mV, even during the largest current flow. Data were displayed on a digital oscilloscope (3091: Nicolet Instrument Corporation, Madison, WI, USA) and stored on video cassettes (Sony PCM–701ES digital audio processor and Sony Betamax SL–T50 ME video cassette recorder) or on the hard disk of the computer (sampling frequency: 14.3 kHz) for later off-line analysis. Sodium current was taken as the peak inward current of the STX-sensitive current obtained by digital subtraction of current traces recorded in normal saline and after application of 1.0×10^{-7} mol l^{-1} STX, and its amplitude was measured from the holding current level. The entire analysis of the properties of the Na^+ current reported in this paper has been made on the STX-sensitive current so obtained, and the current traces presented in the figures (except those of Fig. 1) correspond to this current. All data were expressed as mean±S.E. (when quantified).

Results

Effect of STX on the inward current

Fig. 1 shows that the membrane current recorded under our experimental

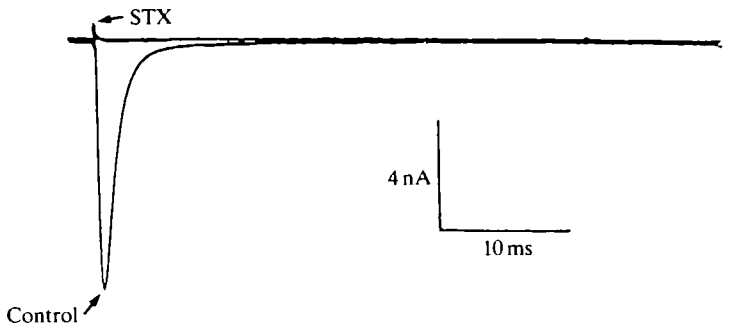

Fig. 1. Blocking effect of 1.0×10^{-7} mol l^{-1} saxitoxin (STX) on the control ionic current elicited with a 50 ms depolarizing pulse to −10 mV applied from a holding potential of −100 mV. Currents are capacity- and leak-corrected.

conditions was entirely blocked by the addition to the superfusing saline of the sodium channel blocker STX at 1.0×10^{-7} mol l^{-1}, indicating that sodium ions flowing through voltage-dependent sodium channels were responsible for it. This effect is in good agreement with our previous observations made in current-clamp mode on the same type of neurone (Lapied *et al.* 1989). Therefore, the sodium current was taken as the peak inward current of the STX-sensitive current.

Current–voltage relationship of the STX-sensitive inward current

Fig. 2Ai shows a typical example of an STX-sensitive Na^+ current from an isolated DUM cell in response to a series of voltage-clamp steps applied from the holding potential of −100 mV. This sodium inward current is voltage- and time-dependent and increasing the depolarizing pulse amplitude accelerates its rates of both activation and inactivation. The peak current–voltage (I–V) relationship obtained in such cells is illustrated in Fig. 2Aii, in which the smooth line represents the best fit to the mean data (N=15) according to the equation (Stühmer, 1988):

$$I_{Na} = G[1 - \{1/\langle 1 + \exp\langle (V - V^a_{0.5})/K^a \rangle \rangle\}](V - V_{rev}), \quad (1)$$

where I_{Na} is the sodium current, V is the membrane potential, $V^a_{0.5}$=−20 mV and K^a=4.03 mV are the activation parameters, G=206 nS is the conductance and V_{rev}=+48.2 mV is the reversal potential. These last two parameters were obtained from the linear regression (correlation coefficient r=0.999) through the data points for potentials more positive than 0 mV.

This representation shows that the sodium inward current starts to activate at around −35 mV, reaches a maximum of 11.08±0.83 nA (N=15) at −10 mV and then decreases to an extrapolated reversal potential of +48.2 mV, very close to the calculated Nernstian equilibrium potential for sodium ions (+47.9 mV).

It should be noted that, under the same experimental conditions, a relatively rare maintained STX-sensitive inward current was observed in about 20 % of the same type of isolated neurones. This maintained inward current persisted during the different applied voltage-clamp pulses (Fig. 2Bi). Both maintained and peak

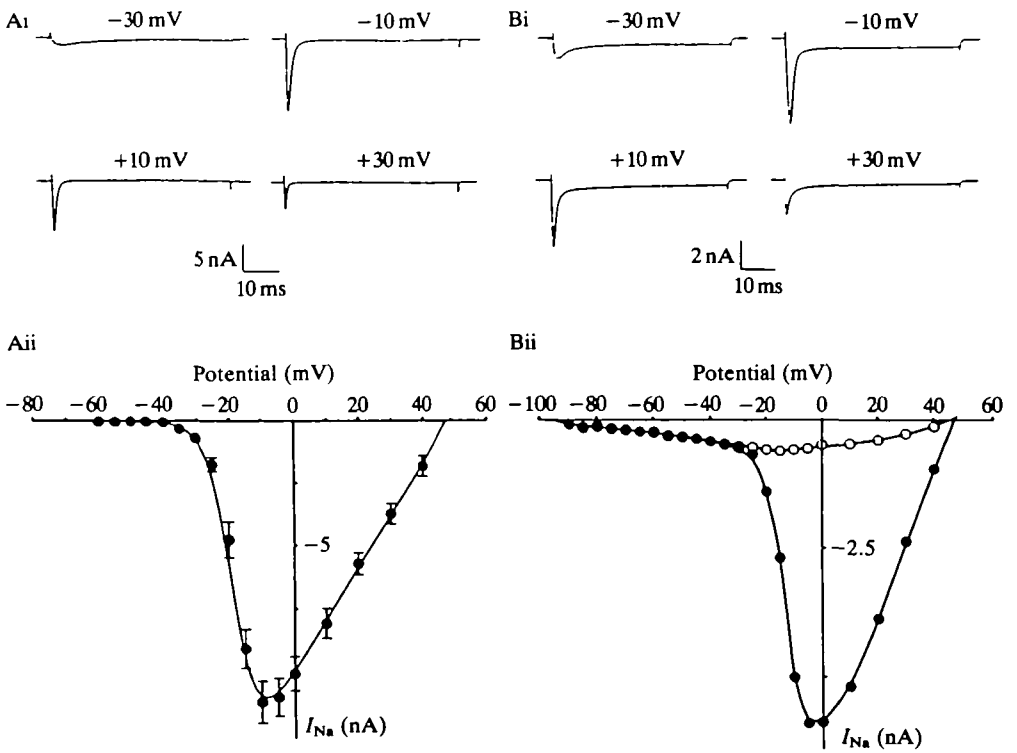

Fig. 2. (A) Typical examples of the most commonly found STX-sensitive Na^+ current (i) recorded at four different potentials indicated above each trace (holding potential −100 mV) and mean current–voltage relationship (ii) of this current. Data points are mean values observed in 15 cells and vertical bars, representing±S.E., are shown when larger than symbols. The smooth curve represents the best fit to the data using equation 1. (B) STX-sensitive Na^+ current recorded in the same conditions in a representative cell having a maintained current at the end of the 50 ms test pulse [potentials indicated above each trace (i), holding potential −100 mV] and corresponding current–voltage relationships (ii). Filled circles correspond to the peak current and open ones to the maintained current at the end of the pulse.

transient inward currents were blocked by 1.0×10^{-7} mol l^{-1} STX, indicating that both were sodium currents (not shown). When the amplitudes of the peaks of the STX-sensitive inward current (which were generally smaller, around 7 nA, than that in the cells showing no maintained current) were plotted against the test potentials, a biphasic curve was observed (Fig. 2Bii). The first part of the curve describes an inward current activating at a very negative potential, around −90 mV, and increasing slightly as the voltage pulses became more positive (up to −30 mV). The second part of the curve corresponds to the 'classical' I–V curve with a maximum at around −5 mV and an extrapolated reversal potential of +46.5 mV, very close to the calculated Nernstian equilibrium potential for sodium ions (+47.9 mV). The I–V relationship of the maintained current (measured at the

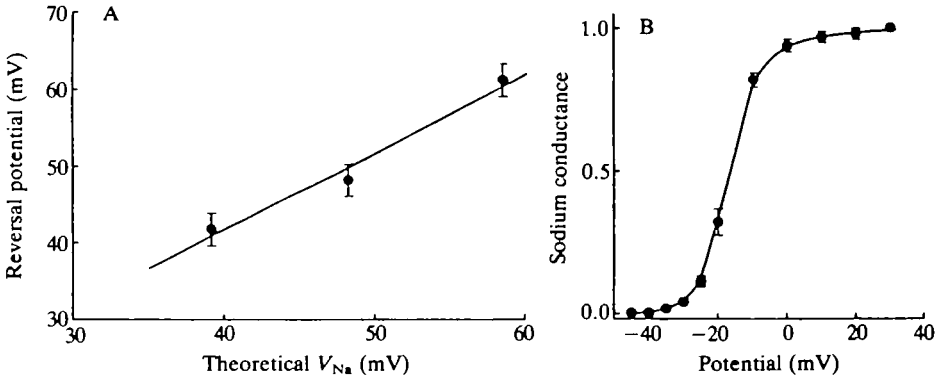

Fig. 3. (A) Reversal potential of the STX-sensitive Na^+ current, measured at three different external Na^+ concentrations (70, 100 and 150 mmol l^{-1}), as a function of the theoretical equilibrium potential for Na^+, calculated from the Nernst equation. Data points are mean values observed in five cells and vertical bars represent ±S.E. The solid line is the linear regression through the data points with a correlation coefficient r=0.99. (B) Voltage-dependence of the normalized conductance (G_{Na}) of the STX-sensitive Na^+ current, calculated according to equation 2.

end of the test pulses) shows that this current increases with more positive potentials. It reaches its maximum amplitude at a potential almost identical to that of the peak sodium current and decreases progressively to the same extrapolated reversal potential (+46.5 mV). However, because this maintained current was only present in about 20% of the neurones, the remaining part of the present study is focused on the properties of the classical inward sodium current present in the majority of the neurones. The detailed study of the properties and kinetics of the maintained current is the topic of a forthcoming paper.

Effect of changing $[Na^+]_o$ on the reversal potential of the STX-sensitive inward current and conductance–voltage relationship

When the external sodium concentration ($[Na^+]_o$) was reduced to 70 mmol l^{-1}, a shift of the reversal potential towards a more negative mean potential of +41.7±2.1 mV (N=5) was observed. By contrast, increasing $[Na^+]_o$ to 150 mmol l^{-1} shifted the reversal potential by +16.4 mV to a mean value of +61.2±2.2 mV (N=5). When the mean values of the reversal potential obtained at different values of $[Na^+]_o$ were plotted against the calculated theoretical sodium equilibrium potential (Fig. 3A) an apparently linear relationship was observed. Linear regression through the data points gave a slope of 1.014±0.153 (correlation coefficient r=0.991), a value that would be expected for a current carried only by sodium ions (assuming that $[Na^+]_i$ remains constant).

Fig. 3B shows the voltage-dependence of the sodium conductance (G_{Na}) calculated (mean±S.E., 15 cells) as a function of the membrane potential according to the equation:

$$G_{Na} = I_{Na}/(V - V_{Na}), \quad (2)$$

where I_{Na} is the transient STX-sensitive inward current, V is the potential at which the membrane is clamped and V_{Na} is the sodium equilibrium potential. G_{Na} increased strongly for test potentials between -40 and $+10$ mV (from 0.305 ± 0.165 nS to 216.63 ± 13.95 nS, $N=15$) and continued to increase slightly at more positive potentials to reach a maximum of 227.11 ± 10.41 nS at around $+30$ mV.

Voltage-dependence of steady-state inactivation and activation

To measure the voltage-dependence of the steady-state inactivation (h_∞) of the STX-sensitive inward current, a conventional two-pulse voltage-clamp protocol was used (Fig. 4A). Inactivation properties were studied by applying a conditioning pulse between -110 and $+30$ mV (in steps of 10 mV) that was long enough (100 ms) to allow the inactivation process to reach its steady-state level. Thereafter, the membrane potential was stepped back to the holding potential (-100 mV) for 1 ms to ensure that the activation variable remained constant, and a 50 ms test pulse was applied to -10 mV, a potential at which the current was almost maximal. The amplitude of the peak inward sodium current decreased as the depolarizing conditioning pulse was made more positive, indicating that fewer channels were available for activation at positive potentials. The inactivation curve, obtained by plotting the amplitude of the peak Na^+ current against the conditioning potential, is shown in Fig. 4B. The smooth line corresponds to the best fit through the mean data points ($N=5$) using a single Boltzmann distribution:

$$h_\infty = 1/\{1 + \exp[(V - V_{0.5})/K]\}\,, \qquad (3)$$

where $V_{0.5}=-41.1$ mV is the potential at which half the sodium channels were inactivated and $K=9.75$ mV corresponds to the slope factor (correlation coefficient $r=0.993$). The steady-state inactivation curve shows that at the resting potential, -52.5 ± 2.4 mV ($N=30$) in these isolated neurones (Lapied *et al.* 1989), about 80 % of the sodium channels are available for activation. Between -100 and 0 mV, h_∞ decreased from 0.989 ± 0.002 to 0.023 ± 0.028 ($N=5$), indicating that all the sodium channels will almost completely inactivate. The fact that the inactivation curve could be fitted by a single Boltzmann distribution indicates that the inactivation time course of the inward sodium current is described by only one exponential function. However, the semilogarithmic plot of $(1-h_\infty)/h_\infty$ against the different conditioning pulses (Fig. 4C) was biphasic: the relationship was linear between -70 and $+30$ mV but deviated from this linearity for potentials more negative than -70 mV. These results strongly suggested that the time course of the inactivation of the sodium inward current was a second-order process (more than a single exponential for relaxation).

The voltage-dependence of the STX-sensitive inward current activation was also studied. The steady-state activation parameter (m_∞) was calculated using the cubic root of the peak conductance measured for each potential, according to the Hodgkin–Huxley formalism of the Na^+ current. No correction was made for current inactivation, as $h_\infty=1$ at the holding potential used (-100 mV; see above).

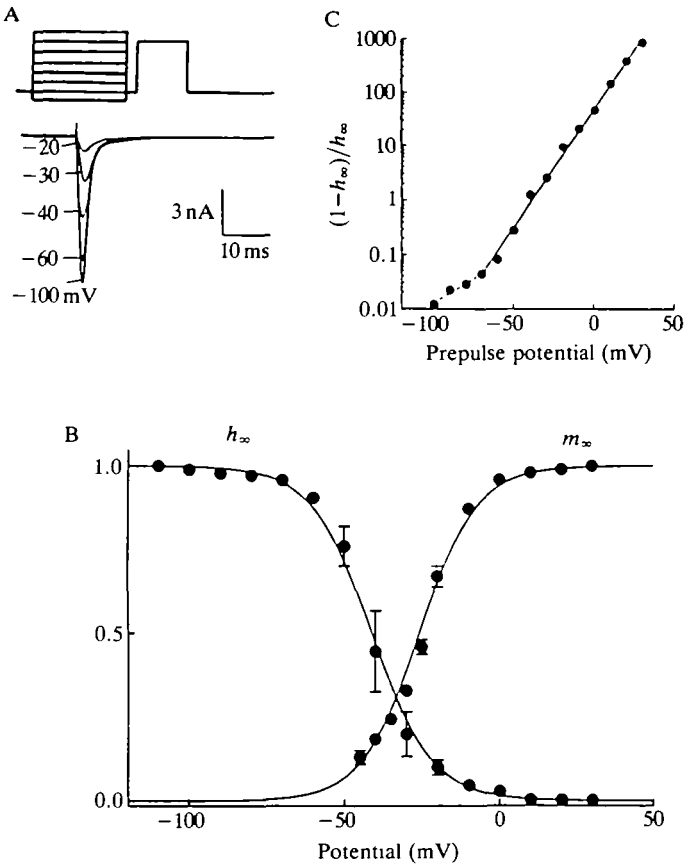

Fig. 4. (A) Voltage-dependent steady-state inactivation of the STX-sensitive Na^+ current studied with the two-pulse voltage-clamp protocol shown above the current traces. Test pulses (50 ms, −10 mV) were preceded by a 100 ms conditioning pulse applied between −110 and +30 mV in steps of 10 mV. Between the conditioning and the test pulses the membrane potential was stepped back to the holding potential (−100 mV) for 1 ms. Prepulse potentials are indicated near each current trace recorded during the test pulse. (B) Voltage-dependence of the Hodgkin–Huxley steady-state inactivation (h_∞) and activation (m_∞) parameters of the STX-sensitive Na^+ current. Data points are mean values observed in five (inactivation) or 15 (activation) cells, and vertical bars, representing ±S.E., are shown when larger than the symbols. Smooth curves were fitted through the data points using single Boltzmann distributions (equations 3 and 4 for h_∞ and m_∞, respectively). (C) Semilogarithmic plot of $(1-h_\infty)/h_\infty$ *versus* prepulse potentials showing the deviation from linearity for potentials more negative than −70 mV.

The m_∞–voltage relationship is given in Fig. 4B, in which the mean values were fitted by a single Boltzmann function of the type:

$$m_\infty = 1/\{1 + \exp[(V_{0.5} - V)/K]\}, \quad (4)$$

where $V_{0.5} = -25.80$ mV is the potential at which half the sodium channels are

Table 1. *Time constants of inactivation of the saxitoxin-sensitive Na^+ current*

Potential (mV)	τ_{h1} (ms)	τ_{h2} (ms)
−25	6.22±0.89	20.69±3.60
−20	2.07±0.54	14.78±1.23
−15	1.10±0.09	10.90±1.30
−10	1.01±0.02	9.29±0.19
−5	0.94±0.04	7.34±1.09
0	0.86±0.04	4.74±0.63
+5	0.77±0.04	4.51±1.01
+10	0.78±0.03	4.49±1.73

Values are means±S.E. of five cells.

activated and K=9.32 mV corresponds to the slope factor (correlation coefficient r=0.995). m_∞ increased steeply in the range of potentials −50 to +10 mV, to reach a maximum at around +30 mV. The h_∞ and m_∞ curves crossed over at approximately −33 mV, a potential at which h_∞ and m_∞ were relatively high (0.3), resulting in a region of $m_\infty - h_\infty$ overlap that extended from approximately −75 to +10 mV. This suggests that a large steady-state window current can be expected.

Kinetics of the STX-sensitive inward current

The kinetic properties of the inward sodium current inactivation were studied using the time course of sodium current decay during a single pulse to different test potentials. For each potential, the decay phase was consistently better fitted by two rather than by one exponential function, indicating that two processes were involved. Both components of inactivation were voltage-dependent and the participation of the fast one increased with increasing test pulse amplitude (e.g. 71.5 % at −20 mV, 91.5 % at 0 mV and 96.7 % at +20 mV). Although there was a very good reproducibility of the values of the fast time constant (τ_{h1}) at all potentials, the values of the slow time constant (τ_{h2}) were scattered for potentials more positive than +10 mV, giving an unclear voltage-dependence. For this reason, we chose to represent the inactivation kinetics by the half-time ($t_{1/2}$) of inactivation, i.e. the time needed for the current to decay from the peak to 50 % of its maximum amplitude. However, it is noteworthy that in the negative potential range τ_{h2} was between three and 10 times larger than τ_{h1}, as shown in Table 1. The curve representing the voltage-dependence of the mean $t_{1/2}$ of inactivation (N=10) is presented in Fig. 5A and was better fitted with two exponentials than one. The $t_{1/2}$ of inactivation decreased steeply for potentials between −25 (10.5±3 ms, N=10) and −10 mV (1.1±0.07 ms, N=10) and then slowly reached its minimum value (0.43±0.07 ms, N=10) at more positive potentials (+35 mV). It should be noted that the values of $t_{1/2}$ of inactivation measured at each potential were very close to τ_{h1}, the fast time constant of inactivation of the Na^+ current (for example, at −10 mV, $t_{1/2}$=1.10±0.07 ms and τ_{h1}=1.01±0.02 ms; at +10 mV,

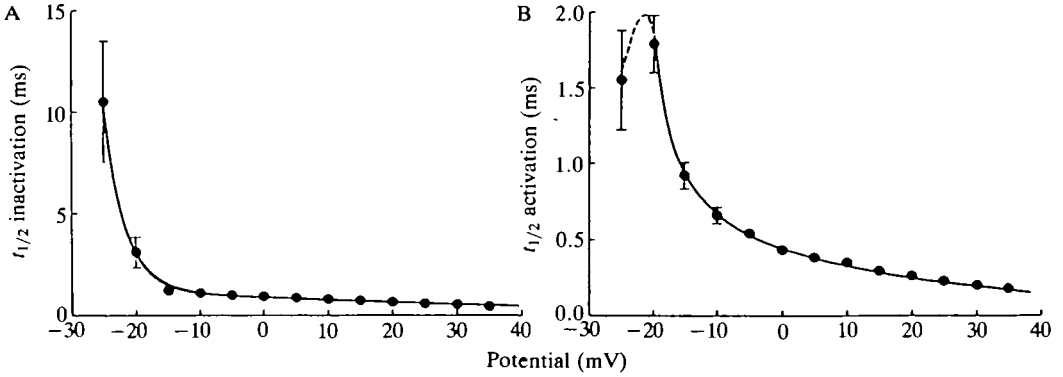

Fig. 5. Voltage-dependences of the half-times of inactivation (A) and of activation (B) of the STX-sensitive Na^+ current. Data points are mean values of 10 cells, and vertical bars, representing±S.E., are shown when larger than the symbols. Solid curves are the best fits to the data points using two exponential functions.

$t_{1/2}$=0.81±0.05 ms and τ_{h1}=0.78±0.03 ms), indicating that the voltage-dependence of $t_{1/2}$ of inactivation reflected that of the fast time constant of inactivation.

Using the same experimental conditions, the global kinetics of the inward sodium current activation was studied. Fig. 5B illustrates the voltage-dependence of the half-time ($t_{1/2}$) of activation, i.e. the time needed for the current to reach 50 % of its maximum peak amplitude. Between −20 and +35 mV the mean values (N=10) of the $t_{1/2}$ of activation were best fitted by two exponential functions. The $t_{1/2}$ of activation reached its maximum value (about 2 ms) at around −20 mV and then decreased for membrane potentials above −20 mV, to approach a minimum of 0.18±0.01 ms (N=10) at +35 mV. In general, the $t_{1/2}$ of activation was 2.5–3 times smaller than the $t_{1/2}$ of inactivation.

Reactivation kinetics of the STX-sensitive inward current

A two-pulse protocol (inset of Fig. 6) was used to determine the rate of recovery from inactivation of the sodium inward current. It consisted of two identical depolarizing pulses applied from the holding potential of −100 mV (or from the recovery potentials) to −10 mV to elicit the sodium current, and separated by a variable time Δt (1–15 ms in steps of 1 ms). The first depolarizing pulse (conditioning pulse) was long enough (8 ms in duration) to give more than 95 % inactivation of the sodium current. Between the two pulses, the membrane was repolarized to three different recovery potentials: −60, −80 or −100 mV (Fig. 6). For each potential, the mean values (5–10 cells) were best fitted by two exponential functions, indicating two processes of reactivation (a fast one and a slow one with respective time constants τ_1' and τ_2'), a finding that is consistent with the two time constants needed to describe the inactivation time course. It appears from these data that the time constants are voltage-dependent (see Table 2), with τ_1' and τ_2' increasing when the holding potential is more positive. It should be noted

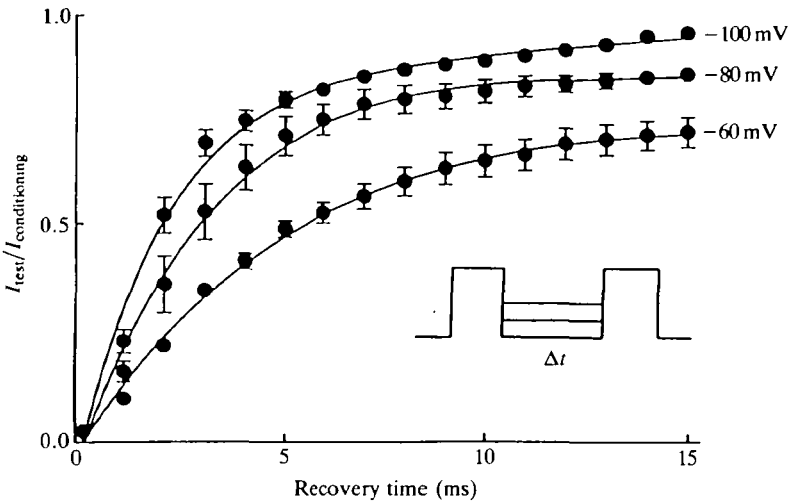

Fig. 6. Time course of recovery from inactivation of the STX-sensitive Na^+ current at three different potentials indicated on each curve. Data points are mean values of five (−80 and −60 mV) or 10 (−100 mV) cells, and vertical bars, representing±S.E., are shown when larger than symbols. Smooth curves through the data points correspond to the best fits using two exponential functions. The inset shows the experimental protocol used. Conditioning and test pulses (8 ms, −10 mV) were respectively applied from −100 mV and from the recovery potential. Δt is the recovery time.

Table 2. *Time constants of recovery from inactivation of the saxitoxin-sensitive Na^+ current*

Potential (mV)	τ'_1 (ms)	τ'_2 (ms)
−100	0.78±0.08	8.40±1.16
−80	1.70±0.07	22.06±1.64
−60	2.79±0.06	31.42±1.70

Values are means±S.E. of 5–10 cells.

that for an identical test pulse (−10 mV), the time constants for recovery from inactivation at −100 mV (τ'_1=0.78±0.08 ms and τ'_2=8.40±1.16 ms, N=10) were very similar to the time constants of inactivation (τ_{h1}=1.01±0.02 ms and τ_{h2}=9.29±0.19 ms, N=5) at the same holding potential.

Discussion

The experiments presented above are the first description of the properties of the STX-sensitive inward current recorded from isolated DUM neurones obtained after dissociation of the dorsal area of the A6 ganglion of the cockroach. They

represent an extension of a previous study concerning the electrical activity (spontaneous action potentials) of these DUM neurones (Lapied *et al.* 1989).

Our results showed that, in the DUM neurones, the inward current examined under voltage-clamp conditions in the whole-cell configuration could be described by the Hodgkin–Huxley model of the Na^+ current (Hodgkin and Huxley, 1952). The inward current recorded under our experimental conditions (i.e. in low-Ca^{2+} saline and in the presence of calcium and potassium channels blockers) was carried by sodium ions flowing through fast voltage-dependent Na^+ channels for the following reasons: (i) it had rapid voltage- and time-dependent rising (activation) and decay (inactivation) phases during depolarization; (ii) it was completely blocked by STX at 1.0×10^{-7} mol l^{-1} (1.0×10^{-9} mol l^{-1} caused about 20% inhibition of the peak current; not shown); and (iii) its reversal potential was very close to and followed the equilibrium potential for Na^+ when the external Na^+ concentration was varied.

In general, the properties of the Na^+ current were similar to those of other invertebrate neurones. The threshold of activation of the Na^+ current was relatively positive (around −35 mV), but similar positive threshold values have been reported in other invertebrate neurones (e.g. *Aplysia*, Adams and Gage, 1979; *Drosophila*, O'Dowd and Aldrich, 1988; Byerly and Leung, 1988) and in vertebrate neurones (e.g. neuroblastoma cells, Quandt and Narahashi, 1984; Ruigt *et al.* 1987; *Xenopus* spinal neurones, O'Dowd *et al.* 1988; rat cervical superior ganglion, Schofield and Ikeda, 1988) as well as in mouse pancreatic β cells (Plant, 1988). Measurement of the voltage-dependence of the steady-state activation and inactivation parameters of the Na^+ current has revealed that complete inactivation of the Na^+ channels of DUM neurones occurred at potentials more positive (+10 mV) than in the majority of these preparations (between −80 and −10 mV). Moreover, the crossing point of the inactivation and activation curves was relatively high (0.3 at −33 mV). As a result, a large $m_\infty - h_\infty$ overlap (from about −70 to +10 mV) was present, giving rise to a large steady-state Na^+ window current that might contribute to the slow predepolarizing phase which characterizes the spontaneous fast action potentials of these neurones (Kerkut *et al.* 1969; Jego *et al.* 1970; Crossman *et al.* 1971; Lapied *et al.* 1989). It should be noted that the values of the threshold (−35 mV) and reversal potentials (+48.2 mV) of the Na^+ current recorded in the majority of these adult neurones were in very good agreement with those of the threshold of the spontaneous action potential (−35.4 mV) and of its overshoot in the presence of TEA^+ (+46.9 mV) recorded in current-clamp mode in the same population of cells (Lapied *et al.* 1989). This confirms that the fast inward Na^+ current was indeed responsible for the action potential upstroke. However, it has been shown that in grasshopper embryos (Goodman and Spitzer, 1981*b*) and in the metathoracic ganglion of the adult locust (Goodman and Heitler, 1979) the action potentials of DUM neurones were carried by both Na^+ and Ca^{2+}. These apparently contradictory observations might suggest a species difference in the ionic dependence of the action potentials. This hypothesis is supported by our findings that the action potentials of adult

cockroach DUM neurones in the A6 ganglion were not suppressed by perfusion with Ca^{2+}-free saline or with Ca^{2+} channel blockers (Lapied *et al.* 1989).

It is noteworthy that the properties of the fast inward current of these DUM neurones are different from those of the Na^+ current recorded in cockroach isolated giant axons (Pichon, 1974). In the former preparation, the kinetics of activation and inactivation of the Na^+ current are about four times slower, the activation threshold 15 mV more positive and complete inactivation of the Na^+ channels occurs at a potential about 50 mV more positive than in the latter preparation. This indicates that, within a species, Na^+ channels of various structures that probably have different functions do not have the same characteristics. It will be important, therefore, to study the Na^+ channels of the DUM cells (which differ from the axonal ones) at the single-channel level to provide evidence of the specific pharmacological properties that are necessary for the understanding of, and perhaps for the discrimination of, the effects of neuroactive molecules (e.g. toxins or insecticides).

An interesting finding was that, in about 20% of the cells, an unexpected maintained current persisted during the whole depolarizing pulse. At present, we have no obvious explanation for this. However, this maintained current was not an artefact (for example, an overcompensation of the leakage current, or remaining Ca^{2+} current, etc.) considering our experimental recording conditions (see Materials and methods for details). Moreover, the biphasic aspect of the current–voltage relationship of the peak current (Fig. 2Bii), together with the observations that the maintained current was (i) STX-sensitive; (ii) voltage-dependent and (iii) had a reversal potential very close to the equilibrium potential for Na^+, strongly suggested that both the peak and the maintained currents might originate from two distinct populations of Na^+ channels, as has been suggested for Ca^{2+} channels (e.g. Nowycky *et al.* 1985). Indeed, Ramaswami and Tanouye (1989) have very recently shown that two genes coding for two different Na^+ channel proteins were present in *Drosophila* genomic DNA. Although two types of Na^+ channels have also been described in the squid and cockroach giant axons (Gilly and Armstrong, 1984; Yawo *et al.* 1985), additional experiments are obviously needed to confirm this hypothesis.

The study of the kinetics of activation and of inactivation of the Na^+ current showed that activation is about three times faster than inactivation. The time to peak of the Na^+ current (assessed by the $t_{1/2}$ of activation) was similar in its voltage-dependence and magnitude to that found in *Drosophila* neurones (O'Dowd and Aldrich, 1988). For example, at 0 mV, the time to peak of the Na^+ current was 0.86 ms at 20°C in the cockroach and about 0.75 ms in *Drosophila* at 19–24°C (see their Fig. 4).

In many voltage-clamp studies, the decay of the Na^+ current during a step depolarization is well fitted by a single exponential relaxation. However, single-channel studies have shown that the molecular processes involved in the inactivation of the macroscopic current are more complicated than suggested by its decay (for a review, see Horn and Vandenberg, 1986). Nevertheless, there are

several studies in which the decay phase of the Na^+ current has been described by two exponential functions (e.g. Schwarz, 1986; Clark and Giles, 1987; O'Dowd *et al.* 1988; Kaneda *et al.* 1989). In the cockroach DUM neurones, we found that the inactivation time course of the Na^+ current was better fitted by the sum of two exponential functions (fast time constant τ_{h1} and slow time constant τ_{h2}), that did not contribute equally to the decay of the current (the participation of the fast component increasing with increasing test pulse amplitude). It should be noted that the values of the $t_{1/2}$ of inactivation of the Na^+ current closely matched those of τ_{h1}, and that they were of the same order of magnitude as the single time constant of inactivation of the Na^+ current of *Drosophila* neurones in culture (O'Dowd and Aldrich, 1988). A possible explanation of the need for two exponentials to describe the decay of the Na^+ current in the cockroach, rather than one, as in *Drosophila*, might be that we studied adult tissue rather than embryonic tissue. This hypothesis is supported by the finding that in *Xenopus* embryonic neurones (O'Dowd *et al.* 1988) the decay phase for young cells can be fitted by a single exponential, whereas two exponentials are needed for older ones. The study of the recovery from inactivation showed that the recovery process occurred in two phases, a fast one and a slow one, and that it was voltage-dependent. These findings are consistent with the need for two exponential functions to describe the inactivation time course. As in other preparations, both time constants increased with increasing recovery potentials, suggesting that positive charges moving through the electric field were involved. However, direct comparison of our results with those found in the literature is not easy because of the large differences in experimental conditions.

Taken together, our results suggest that the behaviour of the Na^+ channels of DUM neurones is more complex than that of the classical Na^+ channels described by the Hodgkin–Huxley model for the following reasons: (i) the steady-state inactivtion was not well fitted by a single Boltzmann distribution in the more negative potential range (Fig. 4C); and (ii) more than one exponential was needed to describe the inactivation time course of the Na^+ current as well as its recovery from inactivation. These findings suggest that in these neurones the Na^+ channel has more than one open state and/or more than one inactivated state. Several models have been proposed to describe the functional properties of the Na^+ channel (e.g. Chiu, 1977; Ochs *et al.* 1981; Sigworth, 1981; Benoit *et al.* 1985) but, at present, we cannot distinguish which model would be better suited to our preparation. A patch-clamp study at the single-channel level should allow a better understanding of the complex properties of the Na^+ channels of these DUM neurones.

BL is supported by a predoctoral fellowship BDI from the CNRS and Région Pays de la Loire.

References

ADAMS, D. J. AND GAGE, P. W. (1979). Characteristics of sodium and calcium conductance

changes produced by membrane depolarization in an *Aplysia* neurone. *J. Physiol., Lond.* **289**, 143–161.

BENOIT, E., CORBIER, A. AND DUBOIS, J. M. (1985). Evidence for two transient sodium currents in the frog node of Ranvier. *J. Physiol., Lond.* **361**, 339–360.

BYERLY, L. AND LEUNG, H. T. (1988). Ionic currents of *Drosophila* neurons in embryonic cultures. *J. Neurosci.* **8**, 4379–4393.

CHIU, S. Y. (1977). Inactivation of sodium channels: second order kinetics in myelinated nerve. *J. Physiol., Lond.* **273**, 573–596.

CLARK, R. B. AND GILES, W. (1987). Sodium current in single cells from bullfrog atrium: voltage dependence and ion transfer properties. *J. Physiol., Lond.* **391**, 235–265.

CROSSMAN, A. R., KERKUT, G. A., PITMAN, R. M. AND WALKER, R. J. (1971). Electrically excitable nerve cell bodies in the central ganglia of two insect species *Periplaneta americana* and *Schistocerca gregaria*. Investigation of cell geometry and morphology by intracellular dye injection. *Comp. Biochem. Physiol.* **40A**, 570–594.

DUNBAR, S. J. AND PITMAN, R. M. (1985). Unitary currents recorded from the soma of identified cockroach neurones using the patch-clamp technique. *J. Physiol., Lond.* **367**, 88P.

DYMOND, G. R. AND EVANS, P. D. (1979). Biogenic amines in the nervous system of the cockroach, *Periplaneta americana*: association of octopamine with mushroom bodies and dorsal unpaired median (DUM) neurones. *Insect Biochem.* **9**, 535–545.

EVANS, P. D. AND O'SHEA, M. (1978). The identification of an octopaminergic neurone and the modulation of a myogenic rhythm in the locust. *J. exp. Biol.* **73**, 235–260.

GILLY, W. F. AND ARMSTRONG, C. M. (1984). Threshold channels – a novel type of sodium channel in squid giant axon. *Nature* **309**, 448–450.

GOODMAN, C. S. AND HEITLER, W. J. (1979). Electrical properties of insect neurones with spiking and non-spiking somata: normal, axotomized, and colchicine-treated neurones. *J. exp. Biol.* **83**, 95–121.

GOODMAN, C. S. AND SPITZER, N. C. (1981*a*). The mature electrical properties of identified neurones in grasshopper embryos. *J. Physiol., Lond.* **313**, 369–384.

GOODMAN, C. S. AND SPITZER, N. C. (1981*b*). The development of electrical properties of identified neurones in grasshopper embryos. *J. Physiol., Lond.* **313**, 385–403.

HAMILL, O. P., MARTY, A., NEHER, E., SACKMANN, B. AND SIGWORTH, F. J. (1981). Improved patch-clamp techniques for high resolution current recording from cells and cell-free membrane patches. *Pflügers Arch. Eur. J. Physiol.* **391**, 85–100.

HODGKIN, A. L. AND HUXLEY, A. F. (1952). A quantitative description of membrane current and its application to conduction and excitation in nerve. *J. Physiol., Lond.* **117**, 500–544.

HORN, R. AND VANDENBERG, C. A. (1986). Inactivation of single sodium channels. In *Ion Channels in Neural Membranes* (ed. J. M. Ritchie, R. D. Keynes and L. Bolis), pp. 71–82, New York: Alan R. Liss, Inc.

HOYLE, G. (1975). Evidence that insect dorsal unpaired median (DUM) neurons are octopaminergic. *J. exp. Zool.* **193**, 425–431.

HOYLE, G. AND DAGAN, D. (1978). Physiological characteristics and reflex activation of DUM (octopaminergic) neurons of locust metathoracic ganglion. *J. Neurobiol.* **9**, 59–79.

JEGO, P., CALLEC, J. J., PICHON, Y. AND BOISTEL, J. (1970). Etude électrophysiologique de corps cellulaires excitables du VIe ganglion abdominal de *Periplaneta americana*. Aspects électriques et ioniques. *C.R. Séanc. Soc. Biol.* **164**, 893–903.

KANEDA, M., OYAMA, Y., IKEMOTO, Y. AND AKAIKE, N. (1989). Scorpion toxin prolongs an inactivation phase of the voltage-dependent sodium current in rat isolated single hippocampal neurons. *Brain Res.* **487**, 192–195.

KERKUT, G. A., PITMAN, R. M. AND WALKER, R. J. (1969). Iontophoretic application of acetylcholine and GABA onto insect central neurones. *Comp. Biochem. Physiol.* **31**, 611–633.

KONINGS, P. N. M., VULLINGS, H. G. B., GEFFARD, M., BUIJS, R. M., DIEDEREN, J. H. B. AND JANSEN, W. F. (1988). Immunocytochemical demonstration of octopamine-immunoreactive cells in the nervous system of *Locusta migratoria and Schistocerca gregaria*. *Cell Tissue Res.* **251**, 371–379.

LANGE, A. B. AND ORCHARD, I. (1984). Dorsal unpaired median neurons, and ventral bilaterally paired neurons, project to a visceral muscle in an insect. *J. Neurobiol.* **15**, 441–453.

LAPIED, B., MALÉCOT, C. O. AND PELHATE, M. (1989). Ionic species involved in the electrical activity of single adult aminergic neurones isolated from the sixth abdominal ganglion of the cockroach *Periplaneta americana*. *J. exp. Biol.* **144**, 535–549.

NOWYCKY, M. C., FOX, A. P. AND TSIEN, R. W. (1985). Three types of neuronal calcium channel with different calcium agonist sensitivity. *Nature* **316**, 440–443.

OCHS, G., BROMM, B. AND SCHWARZ, J. R. (1981). A three-state model for inactivation of sodium permeability. *Biochim. biophys. Acta* **645**, 243–252.

O'DOWD, D. K. AND ALDRICH, R. W. (1988). Voltage-clamp analysis of sodium channels in wild-type and mutant *Drosophila* neurons. *J. Neurosci.* **8**, 3633–3643.

O'DOWD, D. K., RIBERA, A. B. AND SPITZER, N. C. (1988). Development of voltage-dependent calcium, sodium, and potassium currents in *Xenopus* spinal neurons. *J. Neurosci.* **8**, 792–805.

O'SHEA, M. AND EVANS, P. D. (1979). Potentiation of neuromuscular transmission by an octopaminergic neurone in the locust. *J. exp. Biol.* **79**, 169–190.

PFLÜGER, H. J. AND WATSON, A. H. D. (1988). Structure and distribution of dorsal unpaired median (DUM) neurones in the abdominal nerve cord of male and female locusts. *J. comp. Neurol.* **268**, 329–345.

PICHON, Y. (1974). Axonal conduction in insects. In *Insect Neurophysiology* (ed. J. E. Treherne), pp. 73–117. Amsterdam: Elsevier North Holland.

PINNOCK, R. D. AND SATTELLE, D. B. (1987). Dissociation and maintenance *in vitro* of neurones from adult cockroach (*Periplaneta americana*) and housefly (*Musca domestica*). *J. Neurosci. Meth.* **20**, 195–202.

PLANT, T. D. (1988). Na^+ currents in cultured mouse pancreatic β-cells. *Pflügers Arch. Eur. J. Physiol.* **411**, 429–433.

PLOTNIKOVA, S. N. (1969). Effector neurons with several axons in the ventral nerve cord of the asian grasshopper, *Locusta migratoria*. *J. evol. Biochem. Physiol.* **5**, 276–278.

QUANDT, F. N. AND NARAHASHI, T. (1984). Isolation and kinetic analysis of inward currents in neuroblastoma cells. *Neurosci.* **13**, 249–262.

RAMASWAMI, M. AND TANOUYE, M. A. (1989). Two sodium-channel genes in *Drosophila*: Implications for channel diversity. *Proc. natn. Acad. Sci. U.S.A.* **86**, 2079–2082.

RUIGT, G. S. F., NEYT, H. C., VAN DER ZALM, J. M. AND VAN DER BERCKEN, J. (1987). Increase of sodium current after pyrethroid insecticides in mouse neuroblastoma cells. *Brain Res.* **437**, 309–322.

SCHOFIELD, G. G. AND IKEDA, S. R. (1988). Sodium and calcium currents of acutely isolated adult rat superior cervical ganglion neurons. *Pflügers Arch. Eur. J. Physiol.* **411**, 481–490.

SCHWARZ, J. R. (1986). The effect of temperature on Na currents in rat myelinated nerve fibres. *Pflügers Arch. Eur. J. Physiol.* **406**, 397–404.

SIGWORTH, F. J. (1981). Covariance of nonstationary sodium current fluctuations at the node of Ranvier. *Biophys. J.* **34**, 111–133.

STÜHMER, W. (1988). Electrical recordings from cloned sodium channels expressed in *Xenopus* oocytes. In *Molecular Biology of Ionic Channels* (ed. W. S. Agnew, T. Claudio and F. J. Sigworth), pp. 271–276. San Diego: Academic Press Inc.

TANAKA, Y. AND WASHIO, H. (1988). Morphological and physiological properties of the dorsal unpaired median neurons of the cockroach metathoracic ganglion. *Comp. Biochem. Physiol.* **91A**, 37–41.

THOMAS, M. V. (1984). Voltage-clamp analysis of a calcium-mediated potassium conductance in cockroach (*Periplaneta americana*) central neurones. *J. Physiol., Lond.* **350**, 159–178.

WATSON, A. H. D. (1984). The dorsal unpaired median neurons of the locust metathoracic ganglion: neuronal structure and diversity, and synapse distribution. *J. Neurocytol.* **13**, 303–327.

YAWO, H., KOJIMA, H. AND KUNO, M. (1985). Low-threshold, slow-inactivating Na^+ potentials in the cockroach giant axon. *J. Neurophysiol.* **54**, 1087–1100.